Conformational Studies of an *N*-Acylated Hindered Amine Light Stabilizer

Anthony D. DeBellis*

Ciba Specialty Chemicals, Additives Division Research Department, 540 White Plains Road, Tarrytown, New York 10591-9005

Kenneth C. Hass

Ford Research Laboratory, SRL-MD-3028 Dearborn, Michigan 48121-2053

Received: January 22, 1999; In Final Form: April 6, 1999

The low-energy conformations of a commercial, *N*-acylated, hindered amine light stabilizer, Tinuvin 440, are examined both theoretically and experimentally. Candidate structures are determined from an empirical force-field search algorithm and re-optimized using a variety of semiempirical and first-principles quantum chemical methods. The global minimum is robustly predicted to have a twist-boat configuration with the substituted N in its six-membered heterocycle *not* one of the "flagpole" substituents. First-principles Hartree−Fock, post-Hartree−Fock, and density functional theory calculations agree well on the relative stabilities of different conformers, while force-field and semiempirical methods prove unreliable. The present study disagrees with earlier semiempirical results and contradicts their implication that the oxidation and photostabilization behavior of Tinuvin 440 are strongly influenced by a trans-annular, intramolecular hydrogen bond. An alternative boat conformation containing such a bond is predicted by first-principles methods to lie at least 3.4 kcal/mol above the global minimum. NMR and IR spectral data confirm that intramolecular hydrogen bonding plays a negligible role at room temperature and are consistent with the theoretically predicted ground state.

I. Introduction

Hindered amine light stabilizers (HALS) are ubiquitous in their use as additives in polymer and coating stabilization.[1−3] Their utility arises from their purported ability to quench both alkyl and alkylperoxy radicals in a mechanism which regenerates the active stabilizing species. As secondary amines, HALS are somewhat basic compounds and can therefore be rendered inactive through salt formation. This can occur, for example, when acidic cure catalysts are used in a cured coating formulation. In addition, the cure of the coating can be reduced through a titration of the cure catalyst.[4−6] To address these issues, less basic HALS have been developed in an effort to reduce their interactions. Tinuvin 440, **1**, an *N*-acylated HALS, is an example of such a noninteracting stabilizer.

Stabilization via hindered amines involves ultimate oxidation to the nitroxyl radical, which is the primary species involved in the stabilization cycle.[7−10] As a result, oxidation can be a rate-limiting factor in the efficiency and ultimate performance of these compounds. As oxidation occurs at the nitrogen atom, substitution on this atom will certainly have an effect on the rate of this process. It has been suggested that oxidation of *N*-acylated HALS proceeds through the secondary amine.[11,12] As a result, their rate of entry into the HALS stabilization cycle is slowed, and this is manifested by their poorer performance (relative to secondary amines) as light stabilizers.[13−15] Moreover, it has also been suggested that the spirocyclic structure of **1**, in addition to its amidic proton in the hydantoin ring system, is responsible for the existence of an intramolecularly hydrogen bonded (trans-annular) form of the molecule. It has been further implied that this form is even less susceptible to oxidation than similar *N*-acylated HALS which cannot form a trans-annular hydrogen bond such as structures **2** and **3**.[16]

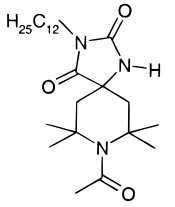

1

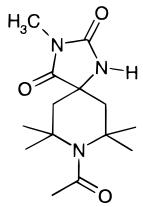

1a

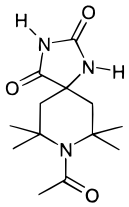

1b

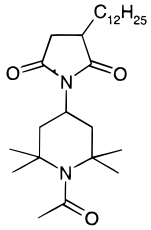

2

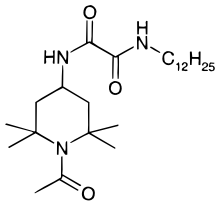

3

In an effort to further understand the factors which influence the stabilization behavior of these compounds, we have undertaken a computational and experimental study of the structure of Tinuvin 440. Due to the relatively large number of possible conformations, we began by obtaining a fairly short list of the low-energy structures of the truncated model compound **1a** using

* Author to whom all correspondence should be addressed. Phone: (914) 785-2949. Fax: (914) 785-3681. E-mail: anthony.debellis@cibasc.com.

10.1021/jp9902654 CCC: $18.00
Published on Web 08/31/1999

TABLE 1: Results of Low-Mode Conformational Search with OPLS/A* Force Field[a]

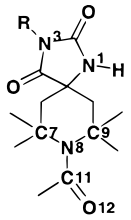

	energy[b]	6-ring[c]	N(1) orientation	C(7,9)−N(8)−C(11)−O(12)	O(12) to N(1) orientation	comments
1[d]	0	twist-R*		−133, +42	syn	
2	0.58	twist-R*		+41, −133	anti	
3	5.04	boat	equatorial	−83, +83	syn	C_s symmetry
4	5.23	chair	equatorial	−78, +104	syn	
5	5.43	chair	axial	−81, +81	syn	C_s symmetry
6	5.70	chair	equatorial	+81, −81	anti	C_s symmetry
7	5.95	twist-boat	axial	−88, +72	syn	trans-annular H-bond
8	6.04	chair	equatorial	+13, −153	anti	slightly distorted chair
9	6.09	chair	axial	−13, +155	syn	slightly distorted chair
10	6.51	chair	axial	+76, −104	anti	

[a] All conformations within 6.5 kcal/mol of global minimum. [b] In kcal/mol, relative to −10.08 kcal/mol for 1. [c] Denotes conformation (and twist orientation) of the six-membered ring. [d] An isoenergetic enantiomeric conformation was found for all structures without C_s symmetry.

an empirical force field. Model **1b** analogues of the resulting structures were used as starting points for semiempirical optimizations so that comparisons could be made with the previous work of Bechtold et al.[16] A variety of first-principles methods and basis sets were subsequently applied to assess the robustness of these results, and to obtain our most reliable estimates of conformer energetics. Finally, NMR and IR spectroscopic data were obtained to provide structural information in solution as well as some experimental verification of our calculations. We conclude, from all available data, that an intramolecularly hydrogen-bonded form of compound **1** is not in fact the lowest energy conformation and plays only a negligible role at room temperature. In addition, we find that predicting the relative energies of low-energy conformations of **1** (as modeled by compounds **1a** and **1b**) proves to be a challenging theoretical problem because of the presence of multiple dipolar groups and a delicate balance involving the orientation of the acetamido group, N-puckering, electrostatic interactions, and steric hindrances.

II. Computational and Experimental Details

Molecular Mechanics Calculations. A conformational search based on the empirical OPLS/A* force field[17] was carried out for model **1a** using MacroModel 6.0.[18] All force-field parameters were either of high or medium quality except for two low-quality torsions and one low-quality angle. Respectively, they were the two equivalent O═C−N−C═O torsions and the C−N−C angle in the hydantoin ring system.

Semiempirical Quantum Calculations. Model **1b** analogues of the lowest-energy molecular mechanics structures were re-optimized using MNDO[19] and AM1,[20] as implemented in MOPAC 6.0. Molecular mechanics corrections for "CONH linkages," which attempt to correct for known deficiencies in semiempirical treatments of amide groups,[21] were included. Test calculations show that these corrections increase the barrier for amide group rotation in acetamide from 3.3 to 20.2 kcal/mol in MNDO and from 9.7 to 19.4 kcal/mol in AM1. For comparison, the density functional theory (DFT) methods below yield corresponding barriers between 17.0 and 19.0 kcal/mol.

First-Principles Quantum Calculations. The same model **1b** analogues of the molecular mechanics results were used as starting points for Hartree−Fock (HF) and DFT geometry optimizations. HF/3-21G and HF/6-31G(d) geometries and MP2/6-31G(d) and hybrid-DFT[22] [B3LYP/6-31G(d) and B3LYP/6-31+G(d,p)] single-point energies were calculated using *Gaussian 94*[23] on a DEC Alphaserver 4000 computer. HF stationary points were characterized by frequency calculations. Local density approximation[24] (LDA) and gradient-corrected DFT geometries were optimized with the parallel version of ADF 2.3[25,26] on an IBM SP computer; these calculations employed a valence double-ζ plus polarization basis of Slater-type orbitals for all elements and a highly accurate numerical integration mesh (parameter 5.0 in ADF). Local minima were determined for the LDA, Becke-Perdew-86 (BP),[27,28] Becke-Lee-Yang-Parr (BLYP),[27,29] and Perdew-Wang-91 (PW)[30] functionals. Selected frequency calculations were performed for the BP functional only. Thermal, basis-set superposition, and zero-point energy corrections were neglected throughout, as they are not expected to have a strong influence on the *relative* stabilities of different conformations.

Experiments. The material 8-acetyl-3-dodecyl-7,7,9,9-tetramethyl-1,3,8-triaza-spiro[4.5]decane-2,4-dione (**1**) was obtained from Ciba Specialty Chemicals Corp., Tarrytown, NY, and used as supplied (Tradename Tinuvin 440); mp 74−78 °C; ^{1}H NMR (499.8493 MHz, $CDCl_3$, δ): 0.89(t, 3H), 1.30 (overlapping multiplets, 20H), 1.56 (s, 6H), 1.62 (s, 6H), 1.92 (d, 2H), 2.22 (s, 3H), 2.43 (d, 2H), 3.48 (t, 2H), 6.00 (s, 1H). Proton NMR spectra were recorded in $CDCl_3$ at room temperature on a Varian UNITY 500 MHz spectrometer. The chemical shifts are reported relative to TMS, where a positive shift is downfield from the standard. Nuclear Overhauser effect (NOE) enhancements were determined by the DNOE technique. FTIR data were obtained in a CCl_4 solvent with a Mattson Polaris spectrometer with 4 cm^{-1} resolution. A NaCl cell of path length 1 mm was used in all cases except the most dilute solution, for which the path length was 10 mm.

III. Computational Results

Molecular Mechanics Calculations. The low-mode conformational search algorithm of Kolossvary and Guida[31] was applied to model **1a** for 2000 steps. This algorithm searches for conformations along low-frequency eigenvectors that are expected to include torsional rotations to different conformers. Each conformation identified for **1a** was found at least 24 times,

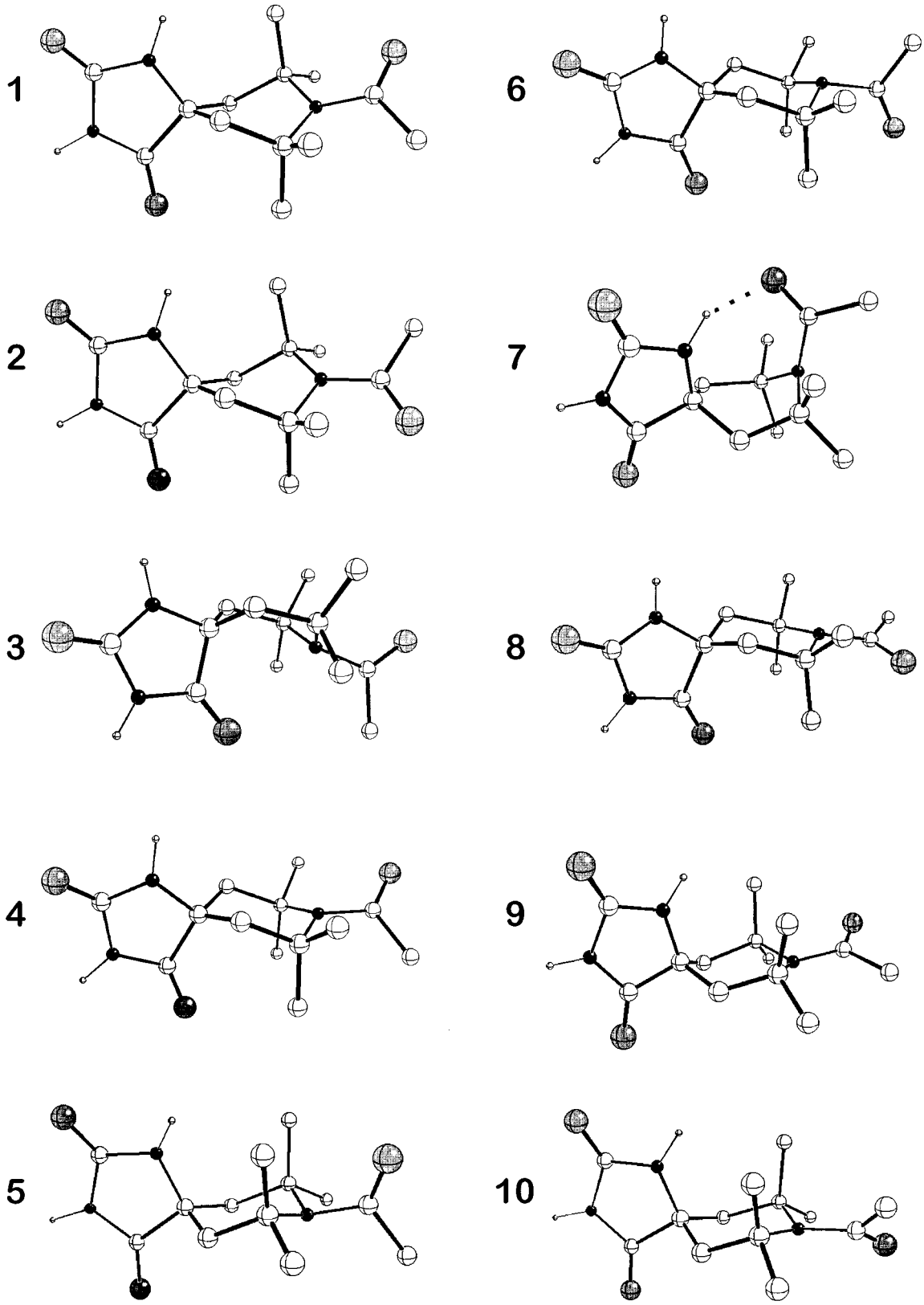

Figure 1. Low-energy conformations of model compound **1b** showing only H atoms associated with N. Atoms C, N, O, and H are depicted as large-open, small-shaded, large-shaded, and small-open spheres, respectively.

which indicates that the search was complete. Table 1 lists all conformations that have energies within 6.5 kcal/mol of the global minimum. Figure 1 shows the analogous structures for model **1b**. The global minimum conformation 1 puts the six-membered heterocycle in a twist-boat configuration in which the "flagpole" substituents are a proton on C(6) (or C(10)) and a methyl group on C(9) (or C(7)). This conformation of the six-membered ring is analogous to the C_2 twist-boat form of cyclohexanone[32] if one substitutes the acetamido group for the carbonyl group of the ketone. Slightly higher in energy is a similar conformation 2 which rotates the acetamido group by 180° relative to conformation 1; its higher energy reflects the

TABLE 2: Semi-Empirical Quantum Results (including molecular mechanics corrections for CONH linkages)[a]

conformer[b]	MNDO heat of formation[c]	C(7,9)−N(8)−C(11)−O(12)	AM1 heat of formation[d]	C(7,9)−N(8)−C(11)−O(12)
1	0.0	−95, +70	0.0	−148, +19
7	1.6	−89, +82	0.0	−46, +96
2	−0.1	+68, −92	0.7	+18, −147
9	optimizes to 5		1.1	−136, +14
5	1.0	−78, +78	1.3	−79, +63
10	3.1	+90, −90	3.4	+139, −61
6	3.5	+77, −77	5.6	+42, −100
4	5.2	−92, +92	7.7	−128, +71
3	optimizes to 1		optimizes to 1	
8	optimizes to 6		optimizes to 6	

[a] Heats of formation in kcal/mol. [b] In order of AM1 heats of formation. Each conformer optimized from the corresponding structure in Table 1. [c] Relative to −86.6 kcal/mol for 1. [d] Relative to −91.7 kcal/mol for 1.

asymmetry induced in the molecule by the twist orientation (R* or S*). The next highest structures are a C_s symmetric boat form 3, a nonsymmetric chair form 4, and two C_s symmetric chair forms 5 and 6, all between 5.0 and 5.7 kcal/mol above the global minimum. The search *does* find an intramolecularly hydrogen-bonded form 7, but its energy lies almost 6 kcal/mol higher than the global minimum. Additional chair forms 8 through 10 are found at still higher energies.

The OPLS/A* force field used in these calculations was originally developed for applications to proteins and has been well validated in that context.[17] However, the accuracy of any empirical force-field description of a system like **1** with multiple dipolar groups is known to be somewhat limited.[33] We have therefore simplified model **1a** further to model **1b,** and have examined the same 10 conformations using more sophisticated quantum-mechanical methods.

Semiempirical Quantum Calculations. We consider both the MNDO method,[19] which was applied previously to **1** in ref 16, and the AM1 method.[20] The latter method was developed primarily to improve on deficiencies in the former, most notably in the description of hydrogen bonding. The results of MNDO and AM1 re-optimizations of the model **1b** analogues of the empirical force field predictions are listed in Table 2. The heats of formation and geometries obtained with these methods are affected only slightly by the inclusion of molecular mechanics corrections for CONH linkages;[21] heats of formation change by less than 1 kcal/mol for all 10 conformers considered, and the most noticeable geometry change is a slight reduction in the puckering of N atoms.

The relative stabilities of the 10 conformers in Table 2 are reasonably similar in the MNDO and AM1 methods, but differ considerably from the molecular mechanics results. Conformers 3 and 8 do not even exist on the semiempirical energy hypersurfaces, and the ordering of chair conformers 4, 5, 6, 9, and 10 is drastically altered. Six different conformations lie within 3.5 kcal/mol of the global minimum in both MNDO and AM1, as opposed to only two in molecular mechanics. The MNDO method finds conformer 2 to be slightly *more* stable than conformer 1, and conformer 7, the "H-bonded" form, to lie only 1.6−1.7 kcal/mol above these most stable twist forms. The AM1 method restores the molecular mechanics ordering of conformers 1 and 2, but further stabilizes conformer 7, making it degenerate with the global minimum. The increased stability of conformer 7 reflects the AM1 method's improved description of hydrogen bonding. Table 3 compares various bond-length predictions for conformers 1 and 7 and shows that the MNDO O(12)−H distance in the latter is far too long to be considered a true intramolecular hydrogen bond. The present MNDO results disagree with those of Bechtold et al., who reported an isoenergetic chair and intramolecularly H-bonded boat form of C_s symmetry;[16] we find that a modification of 7 to impose C_s symmetry produces only a higher-energy saddle point.

TABLE 3: Optimized N−H, C−O, and O•••H Bond Lengths (Å) for Conformers 1 and 7 within Semi-Empirical and First-Principles Methods

	MNDO	AM1	HF	LDA	BP	BLYP	PW
conformer 1							
N(1)−H	0.996	0.987	0.993	1.022	1.018	1.018	1.017
N(3)−H	0.999	0.988	0.996	1.024	1.021	1.021	1.020
C(11)−O(12)	1.224	1.249	1.203	1.228	1.236	1.238	1.234
C(2)−O	1.222	1.242	1.191	1.209	1.218	1.221	1.216
C(4)−O	1.219	1.232	1.190	1.211	1.219	1.222	1.217
conformer 7							
N(1)−H	0.997	0.994	0.999	1.039	1.029	1.027	1.028
N(3)−H	0.999	0.987	0.996	1.025	1.021	1.021	1.020
C(11)−O(12)	1.124	1.243	1.198	1.228	1.233	1.237	1.233
C(2)−O	1.222	1.242	1.190	1.209	1.218	1.221	1.216
C(4)−O	1.220	1.233	1.191	1.211	1.220	1.223	1.218
O(12)−H	3.583	2.159	2.179	1.939	2.143	2.147	2.068

Compared to the molecular mechanics results, all AM1 geometries place the acetamido group more parallel to the plane of the six-membered ring, and all MNDO geometries place it more nearly perpendicular. This can be seen by comparing C(7,9)−N(8)−C(11)−O(12) dihedral angles in Tables 1 and 2. The AM1 preference for a more "planar" orientation is consistent with low-temperature ^{13}C NMR results on similar systems[34] and with the first-principles results below.

First-Principles Quantum Calculations. When tractable, first-principles methods provide the most accurate descriptions of the structures and energetics of complex molecules. First-principles calculations for model **1b** conformers are much more computationally demanding than the above force-field and semiempirical calculations, but are justified in the present context by the unproven ability of the latter methods to balance properly the large number of competing effects that influence the results. To ensure that our first-principles results are themselves robust, we have considered a variety of HF, post-HF, and DFT approaches. Table 4 presents HF/6-31G(d) results for the lowest energy conformations, along with MP2/6-31G(d), B3LYP/6-31G(d), and B3LYP/6-31+G(d,p) single-point energies at the HF/6-31G(d) geometries. HF/3-21G results were also obtained, but are not tabulated because they agree well with the HF/6-31G(d) results (within 1.1 kcal/mol in all cases). The B3LYP calculations with an expanded basis set also support the adequacy of the 6-31G(d) basis. Additional, pure DFT results based on a Slater, instead of Gaussian, orbital basis are presented in Table 5. In these calculations, the geometry of each conformer was fully optimized (without symmetry) for each functional considered. Selected DFT tests with an expanded Slater basis (triple ζ + polarization) yielded results within 0.2 kcal/mol of those in Table 5.

TABLE 4: HF, MP2, and B3LYP Results, at HF/6-31G(d) Geometries[a]

conformer[b]	HF/ 6-31G(d)[c]	MP2/ 6-31G(d)[d]	B3LYP/ 6-31G(d)[e]	B3LYP/ 6-31+G(d,p)[f]
1	0.0	0.0	0.0	0.0
2	1.0	0.8		
9	3.5	3.1	2.8	3.0
7	3.9	3.4	5.1	5.4
5	3.3	5.4		
8	6.7	6.0		
4	10.3	12.1		

[a] Energies in kcal/mol. [b] In order of MP2 energies. All conformers have been characterized as minima at the HF/6-31G(d) level. Vibrational analysis of conformers 3 and 6 produced one or more imaginary frequencies. [c] Relative to −892.499288 au for 1. [d] Relative to −895.203514 au for 1. [e] Relative to −897.993648 au for 1. [f] Relative to −898.058787 au for 1.

There is nearly quantitative agreement among all first-principles methods on the relative energies of the most stable conformers. As in the molecular mechanics and AM1 results, conformer 1 is predicted to be the global minimum, with conformer 2 only slightly higher in energy. The chair conformer 9 is next highest in all except the HF method, in strong disagreement with the molecular mechanics ordering. The first-principles methods predict 9 to be less stable than 1 by 2.8−3.5 kcal/mol, which differs considerably from the 6.1 and 1.1 kcal/mol differences predicted by molecular mechanics and AM1, respectively. The H-bonded boat conformer 7 is the fourth or fifth highest in all of the first-principles methods. It, too, is predicted to be more stable than in the molecular mechanics results and significantly less stable than in the AM1 (and MNDO) results. All first-principles methods place conformer 7 at least 3.4 kcal/mol above the global minimum. At 25 °C, a free energy difference of 3.4 kcal/mol corresponds to a population of less that 0.3% in the higher energy form. The present results thus strongly suggest that a hydrogen-bonded boat form is *not* sufficiently stable to influence the oxidation and stabilization behavior of **1** at room temperature.

The differences that do exist among first-principles predictions, especially for higher energy conformations, are to be expected in view of differences in the treatment of electron exchange and correlation and the different codes and basis sets used for the HF-based and pure DFT results. Results for the three gradient-corrected functionals in Table 5, for example, are generally in better agreement with each other than with LDA results. Quantitative differences in the predicted stability of conformer 7 are largely the result of known difficulties in treating hydrogen bonds.[35−37] The HF and LDA methods, respectively, under- and over-estimate the strengths of such bonds, while the MP2, B3LYP, and pure gradient-corrected DFT methods yield improved accuracy. These trends are apparent in the comparisons of O(12)−H bond lengths for conformer 7 in Table 3. The largest discrepancies between different first-principles methods are in the predictions for conformer 5, whose relative stability varies from 3.3 kcal/mol in HF (making it more stable than conformers 7 and 9!), to 5.4 kcal/mol in MP2, to 7.2−8.0 kcal/mol in gradient-corrected DFT, to 9.9 kcal/mol in LDA. Of the 10 conformers considered, 5 exhibits the largest puckering of the N(8) atom (e.g., nearest-neighbor bonds at angles of ∼40° with respect to the plane of the three neighbors in the BP geometry), which is apparently accompanied by strong correlation effects.

All first-principles geometry optimizations yield nearly the same orientation of the acetamido group in stable conformers. The HF and BP results in Tables 4 and 5, respectively, confirm the tendency already observed in the AM1 results for this group to adopt a more planar orientation compared to the molecular mechanics and MNDO predictions.

For assistance, in interpreting the FTIR data below, Table 6 lists the frequencies calculated with the BP functional for the N−H and C−O stretch modes of model **1b** conformers 1 and 7. The HF method yields qualitatively similar results but tends to overestimate experimental frequencies by roughly 10%. The N(3)−H mode, of course, is an artifact of the H termination of the alkyl chain in **1**. The only significant difference between the predictions for conformers 1 and 7 is the much lower N(1)−H frequency in 7 due to the perturbing effect of the intramolecular hydrogen bond. In contrast, the C(11)−O(12) frequency, which one might also expect to be perturbed in 7, is nearly the same in both conformers. This C−O mode lies significantly below the coupled asymmetric and symmetric C−O stretches in the hydantoin ring. The BP frequency predictions are consistent with the first-principles bond lengths in Table 3, which robustly predict the N(1)−H bond in 7 to be longer than the other N−H bonds and the acetamido C−O bond to be longer than the hydantoin C−O bonds.

IV. NMR Results

NOE Experiments. The excitation of the acetyl methyl protons led to NOE transfer to each of the 7,7- and 9,9-tetramethyl protons with equal intensity (0.52%). This is suggestive of a freely rotating acetyl group on the NMR time scale. Interestingly, the population of an intramolecularly H-bonded form, such as conformer 7, does not preclude the observation of equal NOE enhancements at each set of gem-dimethyl groups. An inspection of a molecular model of conformation 7 and its enantiomer reveals that the inter-proton distances are all essentially equal.

Additionally, NOE transfer was observed between the N−H proton and axial piperidyl gem-dimethyl (0.67%) and methylene (1.68%) protons. This observation is consistent with the population of two chair forms of the molecule, one with an axial N−H (NOE enhancement to the gem-dimethyl protons) and the other with an equatorial N−H (NOE enhancement to the methylene protons). Specific examples would include the ring-

TABLE 5: Density Functional Theory Results, Based on Optimized Geometries for Each Functional[a]

conformer[b]	LDA energy[c]	BP energy[d]	C(7,9)−N(8)−C(11)−O(12)[e]	BLYP energy[f]	PW energy[g]
1	0.0	0.0	−154, +17	0.0	0.0
2	1.6	1.4	+17, −153	1.1	1.3
9	3.3	2.8	−151, +3	2.8	2.9
7	3.4	4.2	−113, +35	4.3	3.7
8	6.0	6.1	−1, −157	5.9	6.2
5	9.9	7.8	−67, +71	7.2	8.0
4	10.7	11.3	−151, +51		
6	9.9	11.8	+72, −66		

[a] Energies in kcal/mol. [b] In order of BP energies. [c] Relative to −5928.28 kcal/mol for 1. [d] Relative to −5456.45 kcal/mol for 1. [e] BP geometry. HF structures had very similar dihedral angles. [f] Relative to −5240.23 kcal/mol for 1. [g] Relative to −5553.67 kcal/mol for 1.

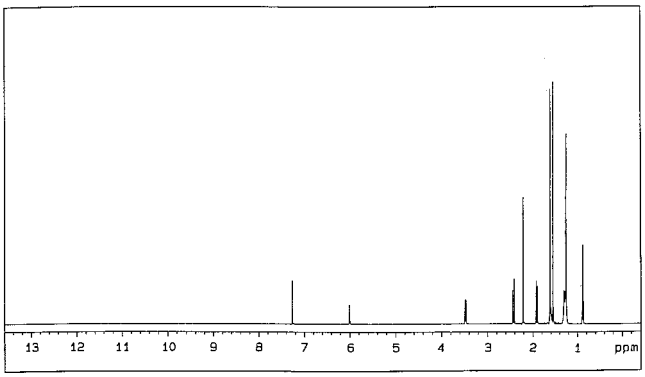

Figure 2. ^{1}H NMR spectrum of **1** at room temperature in $CDCl_3$ solution.

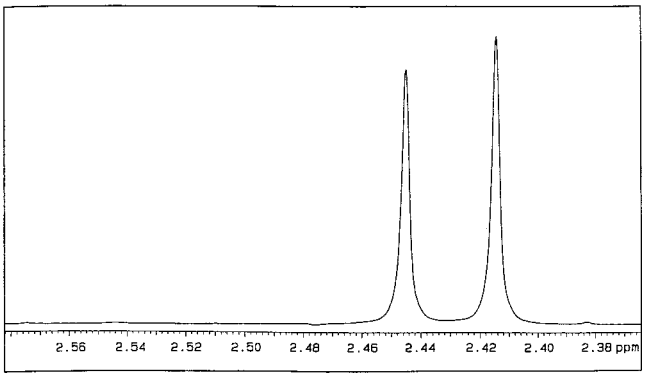

Figure 3. Scale expansion of Figure 2 from 2.37 to 2.58 ppm showing downfield half of AB quartet.

TABLE 6: N−H and C−O Stretch Frequencies (cm^{-1}) Calculated in DFT with BP Functional

mode	conformer 1 frequency	conformer 7 frequency
N(1)−H	3531	3365
N(3)−H	3507	3503
C(11)−O(12)	1645	1648
C(2)−O, C(4)−O (asym)	1755	1752
C(2)−O, C(4)−O (sym)	1793	1789

inverted pairs of conformations 5 and 6, 8 and 9, or 4 and 10. Most importantly, these data are also consistent with the equivalent population of two enantiomeric twist forms, such as the predicted lowest-energy conformations 1 and 2.

Long-Range Coupling. Figure 2 shows the ^{1}H NMR spectrum of **1** at room temperature in $CDCl_3$ solution. Figure 3 is the same spectrum scale expanded to show the downfield half of the AB quartet formed from the methylene protons bonded to carbons six and ten. A geminal coupling $^2J_{HCH}$ of 14.5 Hz is observed. In a rigid system such as conformation 7, one might expect to observe a four-bond long-range coupling to the proton on the opposite side of the six-membered ring.[38] The magnitude of this coupling is expected to be on the order of 1−2 Hz. Since the two equatorial (or axial) protons bonded to carbons six and ten are magnetically equivalent, these atoms would be *virtually* coupled and a splitting would not be observable in the ^{1}H NMR spectrum. This magnetic equivalence is removed when one carbon (six or ten) is replaced by the isotope ^{13}C. This is true for about 1% of the sample. In this case, the equatorial (or axial) protons do not have the same chemical shift, and coupling (if it is operative) can be observed in the ^{13}C satellite sidebands of these signals. Figure 4 shows a further scale expansion of the ^{13}C satellite sidebands ($^1J_{CH}$ = 130 Hz) at 2.544 and 2.574 ppm. As one can see in the figure,

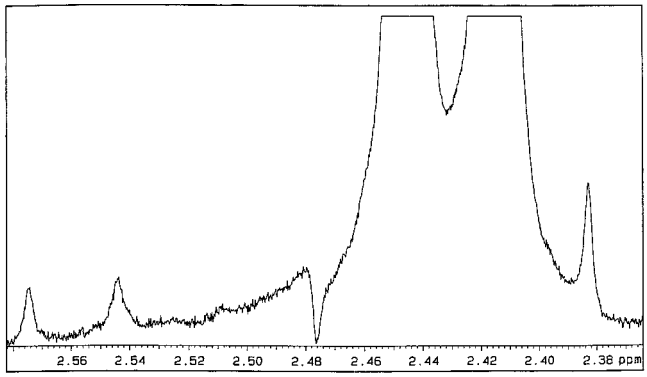

Figure 4. *Y*-axis scale expansion of Figure 3 showing ^{13}C satellite sidebands.

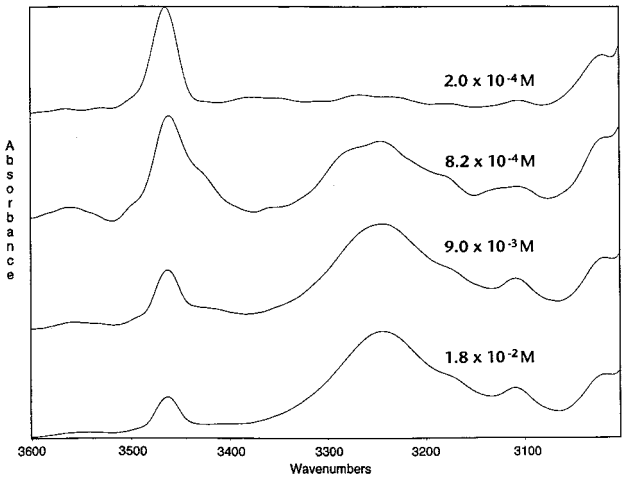

Figure 5. FTIR absorption spectrum of **1** in carbon tetrachloride solution at indicated molar concentrations. High-frequency region.

there is no evidence of coupling to additional nuclei. This result suggests that a fairly rigid conformation is not significantly populated.

V. FTIR Results

More direct evidence for the absence of intramolecular H-bonding in **1** is provided by FTIR spectra obtained in solutions of CCl_4. Figure 5 shows the high-frequency regions of these spectra collected for four concentrations ranging over 2 orders of magnitude from 1.8×10^{-2} to 2.0×10^{-4} M. The absorption at 3464 cm^{-1} is reasonably close to the value predicted in Table 6 for the stretching mode of a free N−H group. The 3245 cm^{-1} mode is assigned to a hydrogen-bonded N−H group on the basis of its downshift and broadening. The ratio of the free to H-bonded peak intensities increases significantly upon dilution. At the lowest concentration, only the free peak remains. This concentration dependence is a classic example of the effects of *inter*molecular hydrogen-bonding. The complete absence of a H-bonded peak in the most dilute solution strongly suggests that the isolated molecule does not spend any appreciable time in an intramolecular H-bonded form like conformer 7 at room temperature.

Figure 6 shows FTIR spectra for the same four solutions in the lower-frequency carbonyl region near 1700 cm^{-1}. Using the results in Table 6, we assign the two high-frequency absorptions to the symmetric and asymmetric stretches of the hydantoin-ring carbonyls, and the lower-frequency band to the isolated carbonyl of the acetamido functionality. The frequencies of the two higher modes shift slightly with concentration, but the

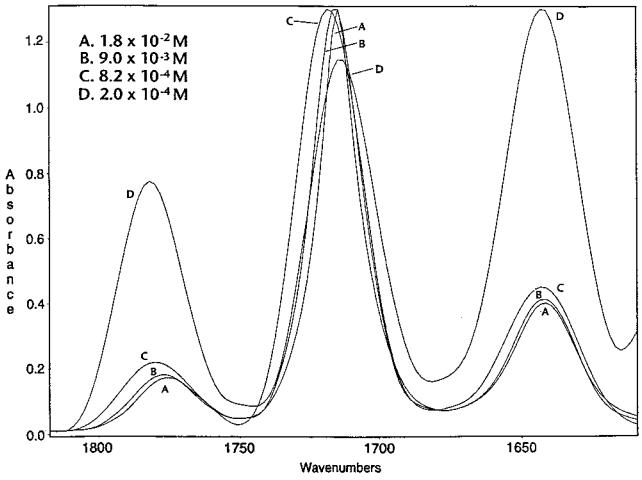

Figure 6. FTIR absorption spectrum of **1** in carbon tetrachloride solution at indicated molar concentrations. Carbonyl region.

frequency of the lower mode remains constant. It is tempting to conclude from this that whatever intermolecular hydrogen bonding is occurring involves only the carbonyls in the hydantoin ring. However, the theoretical results in Table 6 show that even when the acetamido carbonyl is clearly involved in a hydrogen bond (as in conformer 7) its stretch frequency does not necessarily shift appreciably. Nevertheless, we expect that intermolecular hydrogen bonding does occur almost entirely through the hydantoin-ring carbonyls in the lowest energy conformations in Figure 1 because of the greater shielding of the acetamido carbonyl by the bulky methyl groups at the C(7) and C(9) positions.

VI. Conclusions

Of the computational methods considered in this paper, only first-principles quantum calculations provide what appears to be a consistent and satisfactory description of the relative energies of the low-energy conformations of Tinuvin 440. All methods, including molecular mechanics and semiempirical calculations, predict the most stable conformation to be a twist-boat form with the flagpole substituents a proton on C(3) (or C(5)) and a methyl group on C(6) (or C(2)). First-principles HF, post-HF, and DFT calculations place an alternative, intramolecularly hydrogen-bonded form too high in energy to be significantly populated at room temperature. NMR and FTIR data confirm this absence of intramolecular hydrogen bonding and are qualitatively consistent with the theoretically predicted ground state. The present study thus contradicts the claim in ref 16 that Tinuvin 440 may differ in its oxidation and stabilization behaviors compared to other *N*-acylated HALS because it adopts an intramolecularly H-bonded conformation.

Acknowledgment. The authors thank Drs. John Gerlock, Bill Schneider, and Steve Pastor for helpful discussions throughout this work. Additionally, we thank Dr. Ronald Rodebaugh and Sai Shum for their help with the NMR spectral data.

References and Notes

(1) Schirmann, P.; Dexter, M. *Handbook of Coatings Additives*; Marcel Decker Inc.: NewYork/Basel, 1987.
(2) Gachter, R.; Muller, H. *Plastic Additives*; Hanser, C., Ed.; Verlag: Munchen, 1990.
(3) Valet, A. *Light Stabilizers for Paints*; Vincentz, C. R., Ed.; Verlag: Hannover, 1997.
(4) Berner, G.; Rembold, M. *Org. Coat.* **1984**, *6*, 55.
(5) Bramer, D.; Holt, M.; Mar, A. *Polym. Mater. Sci. Eng*. **1990**, *63*, 647.
(6) Valet, A. *Farbe+Lack* **1990**, *96*, 689.
(7) Ivanov, V.; Shlyapintokh, V.; Shapiro, A.; Khvostach, O.; Rozantsev, E. *Izv. Akad. Nauk, Ser. Khim*. **1974**, *8*, 1916.
(8) Carlsson, D.; Grattan, D.; Suprunchuk, T.; Wiles, D. *J. Appl. Polym. Sci*. **1978**, *22*, 2217.
(9) Denisov, E. *Int. Symp. on Degradation of Polymers*, Brussels, 1974, 137.
(10) Klemchuk, P.; Gande, M.; Cordola, E. *Polym. Degrad. Stab*. **1990**, *27*, 65.
(11) Carlsson, D.; Wiles, D. *Polym. Prep*. **1984**, *25*, 24.
(12) Kurumada, T.; Ohsawa, H.; Fujita, T.; Toda, T.; Yoshioka, T. *J. Polym. Sci. Polym. Chem. Ed.* **1985**, *23*, 2747.
(13) Bauer, D.; Gerlock, J.; Mielewski, D.; Paputa Peck, M.; Carter, R. *Polym. Degrad. Stab*. **1990**, *28*, 39.
(14) Bauer, D.; Gerlock, J.; Mielewski, D. *Polym. Degrad. Stab*. **1990**, *28*, 115.
(15) Bauer, D. *J. Coat. Tech*. **1994**, *66*, 57.
(16) Bechtold, K.; Hess, E.; Lignier, G. *Farbe+Lack* **1993**, *99*, 25,
(17) Jorgensen, W. L.; Tirado-Rives, J. *J. Am. Chem. Soc*. **1988**, *110*, 1657.
(18) Mohamadi, F.; Richards, N. G. J.; Guida, W. C.; Liskamp, R.; Lipton, M.; Caufield, C.; Chang, G.; Hendrickson, T.; Still, W. C. *J. Comput. Chem*. **1990**, *11*, 440.
(19) Dewar, M. J. S.; Thiel, W. *J. Am. Chem. Soc*. **1977**, *99*, 4899, 4907.
(20) Dewar, M. J. S.; Zoebisch, E. G.; Healy, E. F.; Stewart, J. J. P. *J. Am. Chem. Soc*. **1985**, *107*, 3902.
(21) MOPAC manual, available from QCPE, Creative Arts Building 181, Indiana University, Bloomington, IN 47405.
(22) Becke, A. D. *J. Chem. Phys.* **1993**, *98*, 1372.
(23) Frisch, M. J.; Trucks, G. W.; Schlegel, H. B.; Gill, P. M. W.; Johnson, B. G.; Robb, M. A.; Cheeseman, J. R.; Keith, T. A.; Petersson, G. A.; Montgomery, J. A.; Raghavachari, K.; Al-Laham, M. A.; Zakrzewski, V. G.; Ortiz, J. V.; Foresman, J. B.; Cioslowski, J.; Stefanov, B. B.; Nanayakkara, A.; Challacombe, M.; Peng, C. Y.; Ayala, P. Y.; Chen, W.; Wong, M. W.; Andres, J. L.; Replogle, E. S.; Gomperts, R.; Martin, R. L.; Fox, D. J.; Binkley, J. S.; Defrees, D. J.; Baker, J.; Stewart, J. P.; Head-Gordon, M.; Gonzalez, C.; Pople, J. A. *Gaussian 94 (Revision E.2)*; Gaussian, Inc.: Pittsburgh, PA, 1995.
(24) Vosko, S. H.; Wilk, L.; Nusair, M. *Can. J. Phys.* **1980**, *58*, 1200.
(25) Baerends, E. J.; Ellis, D. E.; Ros, P. *Chem. Phys.* **1973**, *2*, 41.
(26) te Velde, G.; Baerends, E. J. *J. Comput. Phys.* **1992**, *99*, 84.
(27) Becke, A. D. *Phys. Rev. A* **1988**, *38*, 3098.
(28) Perdew, J. P. *Phys. Rev. B* **1986**, *33*, 8822.
(29) Lee, C.; Yang, W.; Parr, R. *Phys. Rev. B* **1988**, *37*, 785.
(30) Wang, Y.; Perdew, J. P. *Phys. Rev. B* **1991**, *44*, 13298.
(31) Kolossvary, I.; Guida, W. C. *J. Am. Chem. Soc*. **1996**, *118*, 5011.
(32) Burkert, U.; Allinger, N. L. *Molecular Mechanics*, ACS Monograph 177, American Chemical Society: Washington, DC, 1982; p 212.
(33) Dosen-Micovic, L.; Jeremic, D.; Allinger, N. L. *J. Am. Chem. Soc*. **1983**, *105*, 1716.
(34) Lunazzi, L.; Macciantelli, D.; Tassi, D.; Dondoni, A. *J. Chem. Soc., Perkin II* **1980**, 717.
(35) Sim, F.; St.-Amant, A.; Papi, I.; Salahub, D. R. *J. Am. Chem. Soc.* **1992**, *114*, 4391.
(36) Novoa, J. J.; Sosa, C. *J. Phys. Chem.* **1995**, *99*, 15837.
(37) Hass, K. C.; Schneider, W. F.; Estévez, C. M.; Bach, R. D. *Chem. Phys. Lett.* **1996**, *263*, 414.
(38) Abraham, R. J.; Loftus, P. *Proton and Carbon-13 NMR Spectroscopy*; Heyden & Son Ltd.: London, 1978; p 49.